

Chapter 3

MATERIALS AND METHODS

3.1 Materials

3.1.1 Gamma Spectrometry System (Fig. 3.1)

The system composes of these following components:

- 3.1.1.1 CANBERRA high-purity detector (close end co-axial type) including vertical cryostat and preamplifier energy range 50 keV -20 MeV, 20 % relative efficiency, Full Width at Half Maximum at 1332 keV : 1.9 keV
- 3.1.1.2 Amplifier : CANBERRA Model 2022
- 3.1.1.3 High voltage power supply : CANBERRA
- 3.1.1.4 Multichannel analyser : CANBERRA SERIES 35 plus Model 3503
- 3.1.1.5 Computer 16 bits : IBM AT02 personal computer with 512 kB memory
- 3.1.1.6 Lead shield with thickness of 100 mm, 2 mm copper lining, 315 mm diameter x 400 mm height, low level activity : CANBERRA Model EO 15202
- 3.1.1.7 LN₂ Monitor: CANBERRA Model CE 1786
- 3.1.1.8 SPECTRAN PC: PC/SPECTRAN F Software for gamma ray spectroscopy for use with HPGE detector



Figure 3.1 Gamma Spectrometry System.

3.1.2 Sample and Standard Material Counting Container:

Plastic petri dish (72 mm in diameter and 10 mm. in height) (Fig. 3.2)

3.1.3 Standard Materials and Samples :

- 3.1.3.1 Standard uranium ore (IAEA/RGU-1)
- 3.1.3.2 Standard thorium ore (IAEA/RGTh-1)
- 3.1.3.3 Standard Potassium (IAEA/RGK-1)
- 3.1.3.4 Standard U_3O_8
- 3.1.3.5 Twenty five samples of lignite, three samples of bottom ash and three samples of fly ash collected from Mae Moh Operation Mine and Mae Moh Power Station, Mae Moh, Lampang Province

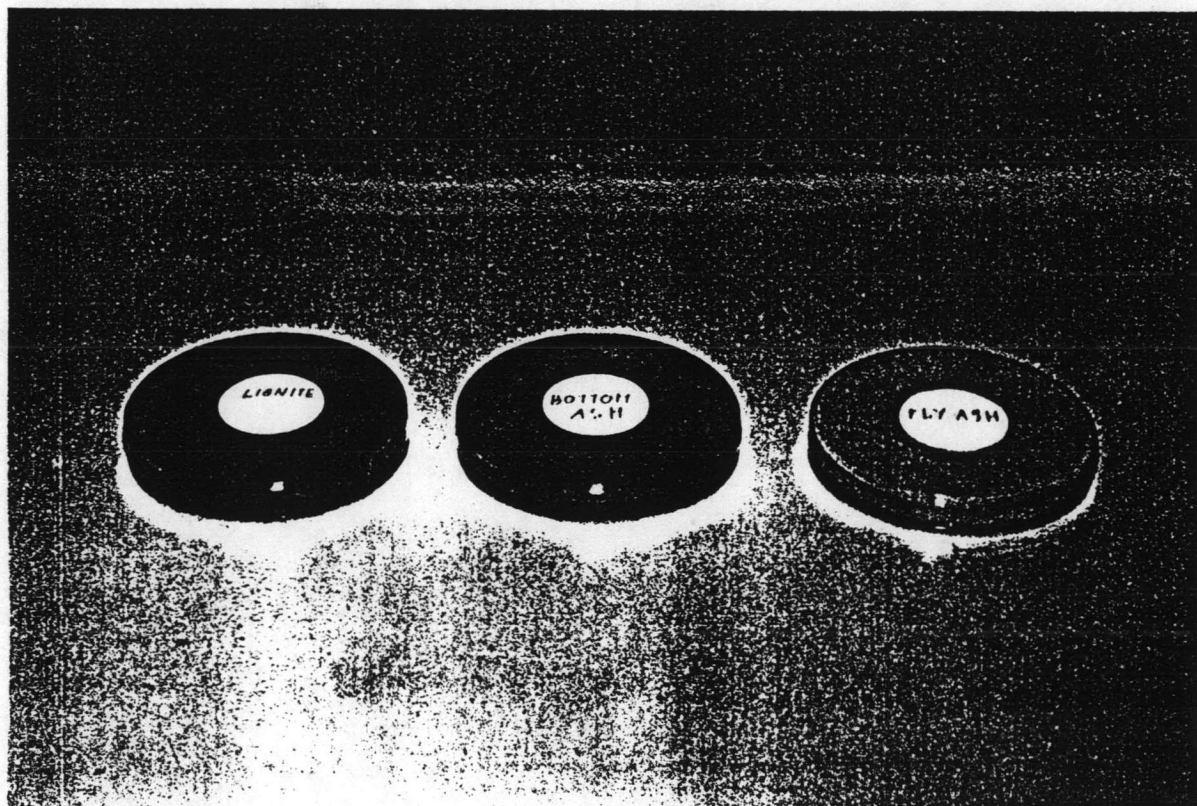


Figure 3.2 Sample and Standard Counting Container

3.2 Method of Measurement

Direct measurement of gamma radiation from coal or lignite is a convenient method for determining its radionuclide contents. Apart from avoiding expensive chemical separation and possible uncertainties arising from losses during processing, direct radiation spectrometry has the advantage of permitting large samples to be used and thus reducing sampling uncertainties. (7)

3.2.1 Preparation of Standard Sources

The standard sources were dried at $110 \pm 10^\circ \text{C}$ in an oven until the constant weight is reached. Then they were transferred to the plastic petri dishes and sealed. They were kept for three weeks prior to the measurement to ensure secular equilibrium between radon and its daughters.

3.2.2 Preparation of Samples

The samples were prepared in the same way as the standard sources.

3.2.3 Energy Calibration

Energy calibration was performed using the calibration option of the SPECTRAN-F program. Peaks regions were selected in the MCA spectrum by setting intensified regions of interest around the peaks to be used. Four channels of background from each side of the peak were included.

Energy versus channel :

$$E = A_1 x C^2 + A_2 x C + A_3$$

where

E = energy in keV

C = channel number

A_1, A_2, A_3 = coefficients determined from fit, where

A_1 is the "offset" in keV

A_2 is the "gain" (or slope) in keV/ch

A_3 is the "non-linearity" in keV/ch²

The typical germanium detector energy calibration curve is shown in Figure 3.3.

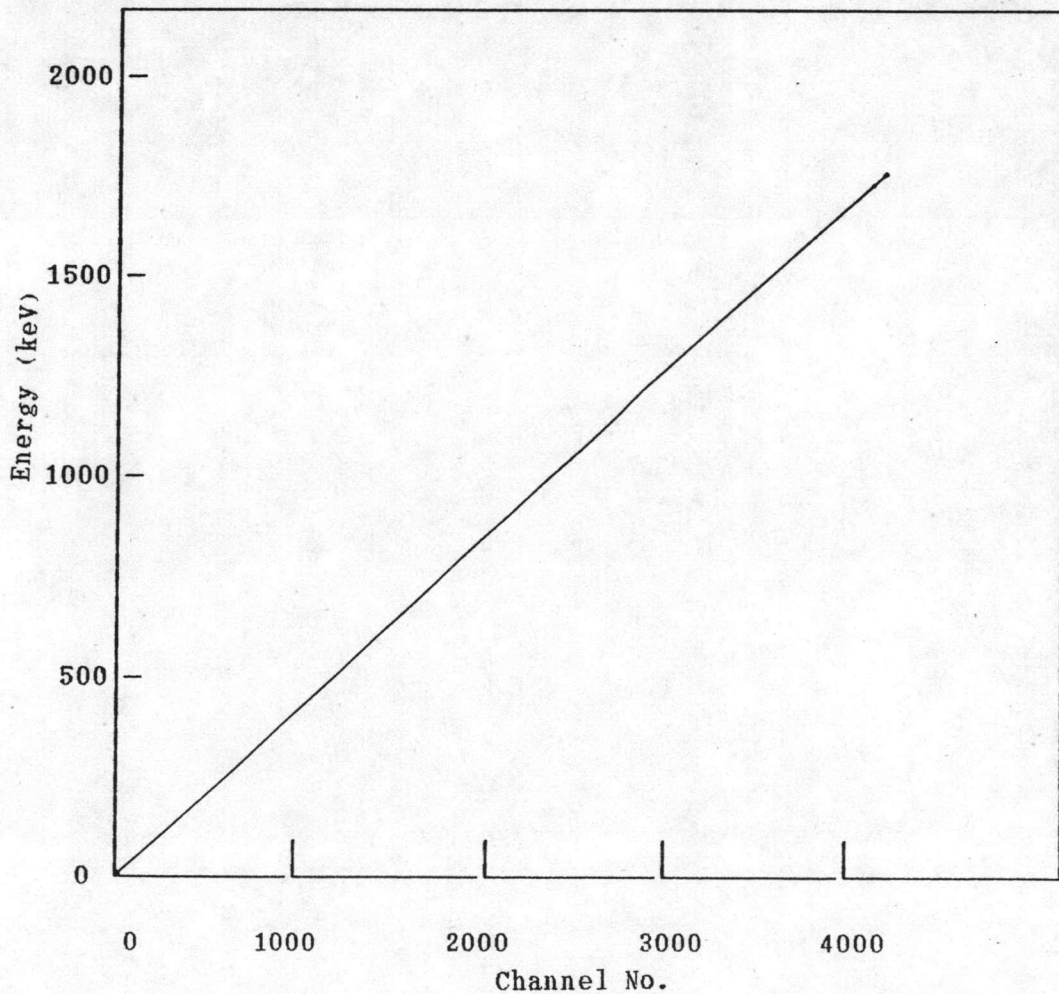


Figure 3.3 Typical Germanium Detector Energy Calibration Curve

3.2.4 Efficiency Calibration

The absolute detection efficiency of a close-end coaxial germanium detector has a maximum value between 80 keV and 100 keV⁽²⁰⁾ decreasing for gamma rays above and below this energy range. (Fig. 2.4)

3.2.5 Determination of Radionuclides in Samples

3.2.5.1 Lignite samples

In lignite U-238, Ra-226, Pb-210, Th-232, Ra-228, Th-228 and K-40 can be detected by gamma spectrometry of their own radiations or those of their decay products.^(10, 11, 30-32) However, for sample with low activity, the peaks used for determining are to be selected carefully. In this experiment, photopeaks at 352 and 609 keV of Pb-214 and Bi-214 respectively, were selected to represent U-238. For Th-232, peaks at 583 keV of Tl-208 and 911 keV of Ac-228 were selected. In the case of K-40, its own peak at 1461 keV was used.

3.2.5.2 Bottom ash and fly ash samples

The radioactivity in bottom ash and fly ash is much higher than that of lignite. Since the secular equilibrium in ash may not be obtained, the certain peaks of particular nuclide of interest were used.

3.2.6 Procedure

3.2.6.1 Energy calibration

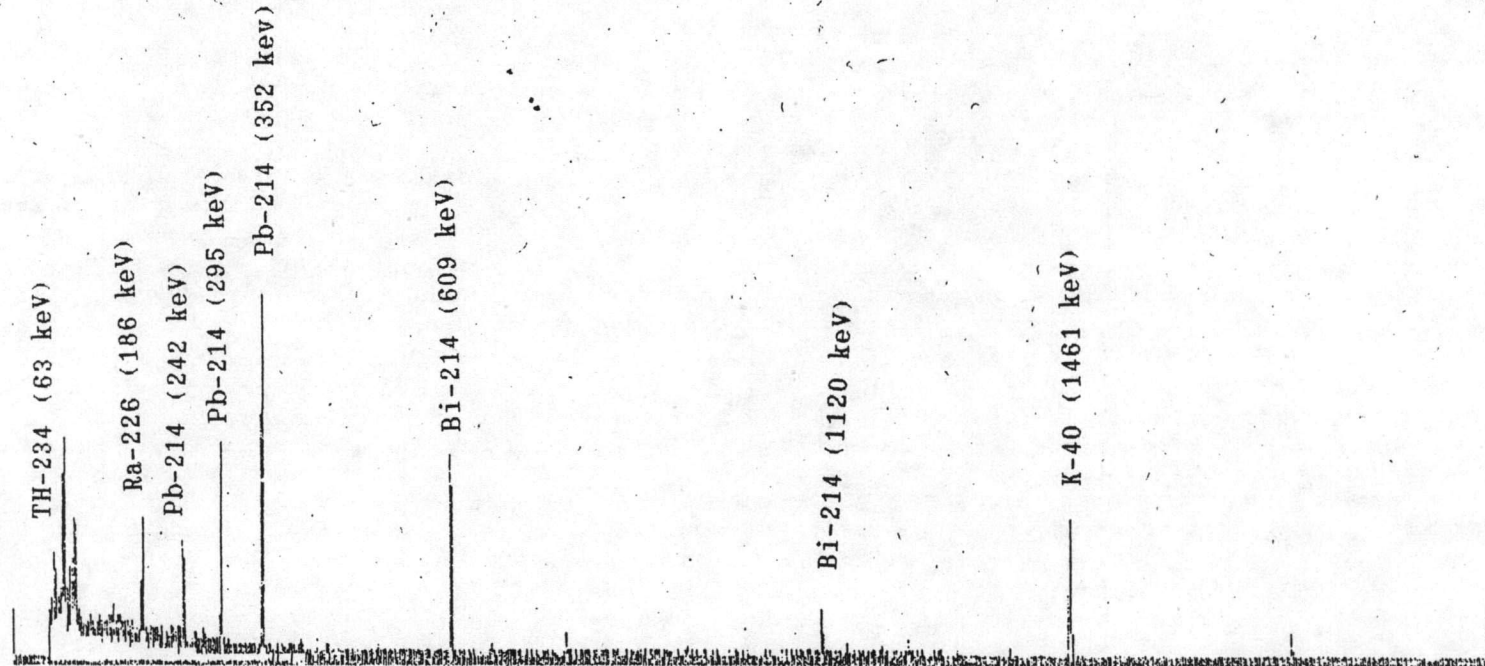
The IAEA uranium ore (IAEA/RGU-1) and the IAEA standard potassium (IAEA/RGK-1) were counted together for 2000 seconds (Figure 3.4). Peaks were selected and intensified (Table 3.1) and then by using the SPECTRAN-F program, the calibration coefficients were

EN CAL

HFS: 0 - 4095

VFS: 1K

AI/LOG EUC/MANUAL



CL= CH# 2
COUNTS 0

FROM CH# 2
ROI# 0 INT 42210

TO CH# 4095
AREA 41698

PSET(L) 1200
ELAP(L) 1200

Figure 3.4 Gamma-ray Spectrum of IAEA RG/U-1 (Uranium Ore)
and IAEA/RGK-1 (Potassium Sulfate)

obtained as follows :

$$\text{Energy} = 3.5758 + 4.9954 \times 10^{-1} \times (\text{ch.no.}) + 2.3592 \times 10^{-8} \times (\text{ch.no.})^2$$

$$\text{FWHM} \times \text{Gain} = 1.4704 + 5.1187 \times 10^{-5} \times (\text{keV}) + 5.0448 \times 10^{-7} \times (\text{keV})^2$$

$$\text{Tailing} \times \text{Gain} = 1.0246 + 1.1612 \times 10^{-4} \times (\text{keV})$$

Table 3.1 The peaks used in energy calibration.

Peak no.	Rdionuclide	Energy (keV)
1	Th-234	63
2	Ra-226	186
3	Pb-214	242
4	Pb-214	295
5	Pb-214	352
6	Bi-214	609
7	Bi-214	1120
8	K-40	1461

This energy calibration was repeated daily to minimize the error arising from the shifts in position of energies.

3.2.6.2 Efficiency calibration

The IAEA uranium ore (IAEA/RGU-1) was counted for 2000 seconds (the spectrum is shown in Figure 3.5). Peaks and other parameters used in efficiency calibration were shown in Table 3.2.

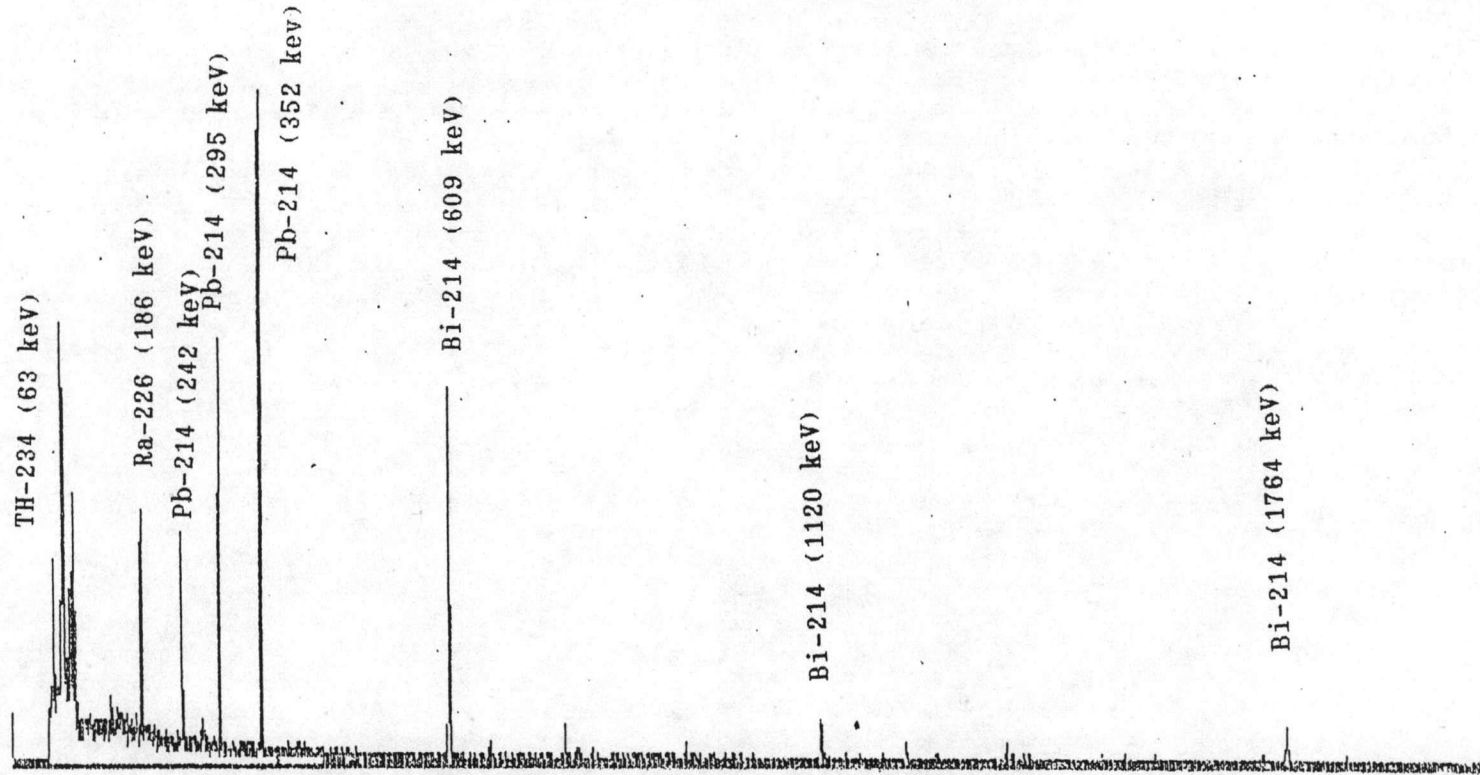
IAEA/RGU-1

HFS: 0 - 4095

VFS: 1K

QIV/LOG

PLU/MANUAL



CL= CH# 2
COUNTS 0

FROM CH# 2
ROI# 0

INT 52603

TO CH# 4095

AREA 51067

PSET(L) 1000

ELAP(L) 1001

Figure 3.5 Gamma-ray Spectrum of IAEA/RGU-1 (Uranium Ore)

Table 3.2 Parameters Used in Efficiency Calibration

Peak no.	Energy (keV)	Radionuclide	Activity (Bq)	Yield	Half-life* (Year)
1	63	Th-234	232.7485	0.057	4.5×10^4
2	186	Ra-226	232.7485	0.04	1600
3	242	Pb-214	232.7485	0.076	1600
4	295	Pb-214	232.7485	0.19	1600
5	352	Pb-214	232.7485	0.36	1600
6	609	Bi-214	232.7485	0.412	1600
7	1120	Bi-214	232.7485	0.136	1600
8	1764	Bi-214	232.7485	0.158	1600

* Since the intermediate products were in equilibrium with their parent, they decayed with the half lives of their parent.

The efficiency curve and some of the efficiency values of interest are shown in Figure 3.6 and Table 3.3 respectively.

The efficiency was checked repeatedly in order to ensure the best results by using different reference materials. The results are shown in Table 4.1-4.3.

3.2.6.3 Background measurement

The background radiation was counted for 18,000-36,000 seconds once a week. The spectrum is shown in Fig. 3.7.

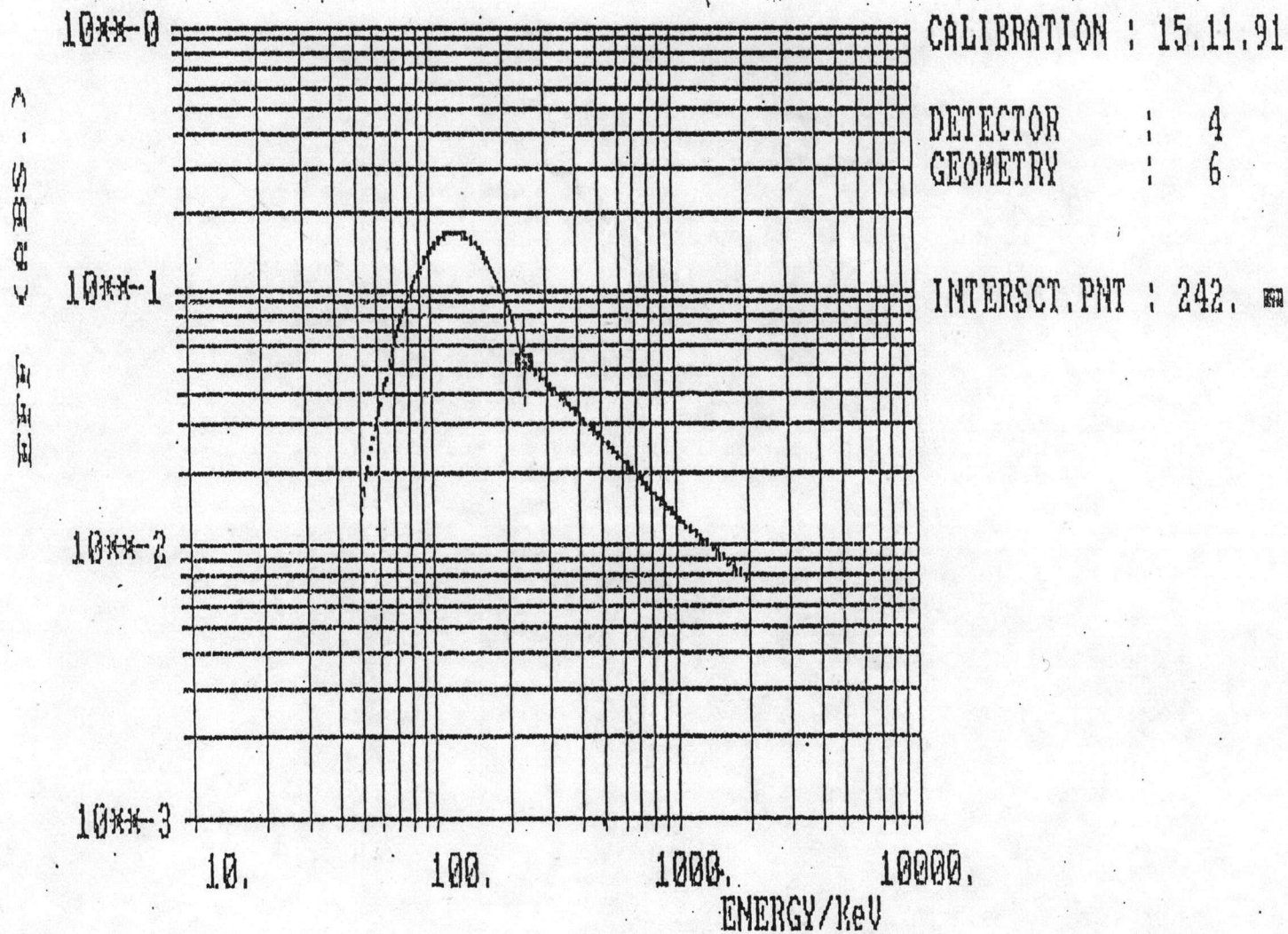


Figure 3.6 Efficiency Curve of Gamma Spectroscopy System

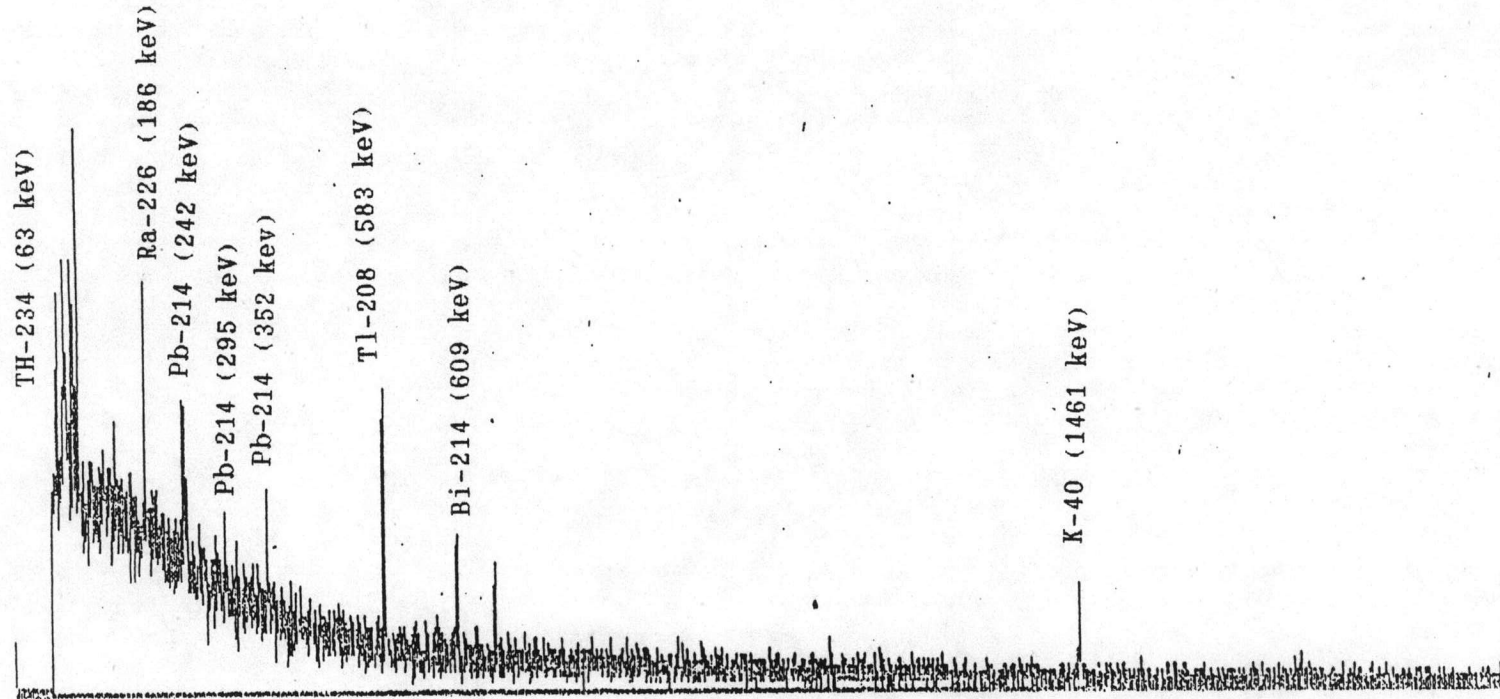
9864 BK

HFS: 0 - 4095

VFS: 256

AN/LOG

TIME/MANUAL



CL= CH# 2
COUNTS 0

FROM CH# 2 TO CH# 4095
ROI# 0 INT 52182 AREA 49623

PSET(L) 40502
ELAP(L) 40509

Figure 3.7 Gamma-ray Spectrum of Background

Table 3.3 The efficiency values at different energy

Energy (keV)	Radionuclide	Efficiency
63	Th-234	4.0864×10^{-2}
186	Ra-226	1.1184×10^{-1}
239	Pb-212	5.4925×10^{-2}
352	Pb-214	3.7055×10^{-2}
583	Tl-208	2.2687×10^{-2}
609	Bi-214	2.1735×10^{-2}
911	Ac-228	1.47160×10^{-2}
1461	K-40	9.6230×10^{-3}

3.2.6.4 Lower limit of detection (LLD)

When all other parameters are fixed, LLD varies with the counting time. In this experiment, the counting time for samples were 18,000-40,000 seconds. The LLD values for 18,000 and 36,000 seconds are shown in Table 3.4. The calculated values were based on error quotation at 1 sigma and at 3.0% confidence level.

Table 3.4 Lower Limit of Detection for 18,000-36,000 Seconds.

Counting time (sec)	Bq/kg (at energy in keV)				
	352	609	583	911	1461
18,000	2.4	2.4	3.6	4.7	15.7
36,000	1.6	1.8	2.4	3.4	9.9

3.2.6.5 Sample measurement

Each of sample was counted, after the secular equilibrium was obtained, between 18,000-36,000 seconds, depending on its activity so as to give a good appraisal on the counting errors. The measurement of each sample was done at least twice.

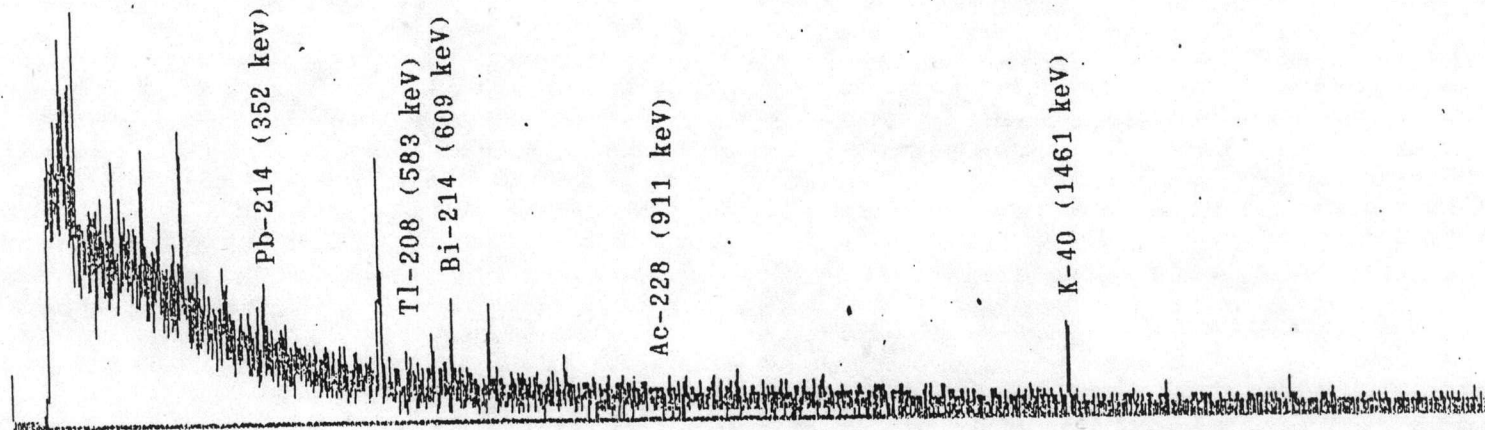
The spectra of lignite , bottom ash and fly ash samples are shown in Fig.3.8-3.11. The results are shown in Table 4.4-4.10.

HPS: 0 - 4095

VFS: 256

IN/LOG

TIME/MANUAL



CL= CH# 2
COUNTS 0

FROM CH# 2
ROI# 0 INT 46895

TO CH# 4095
AREA 42801

PSET(L) 36000
ELAP(L) 35998

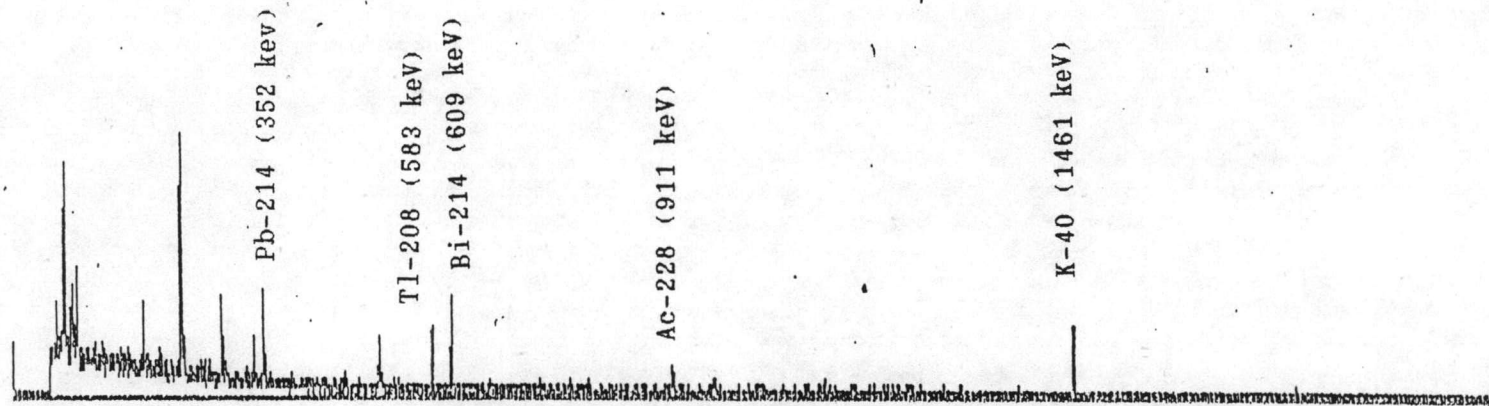
Figure 3.8 Gamma-ray Spectrum of Lignite Sample (Ash = 17.1%)

HFS: 0 - 4095

VFS: 1K

RAW/LOG

LINE/MANUAL



CL= CH# 2
COUNTS 0

FROM CH# 2
ROI# 0 INT 41071

TO-CH# 4095
AREA 40559

PSET(L) 18000
ELAP(L) 18000

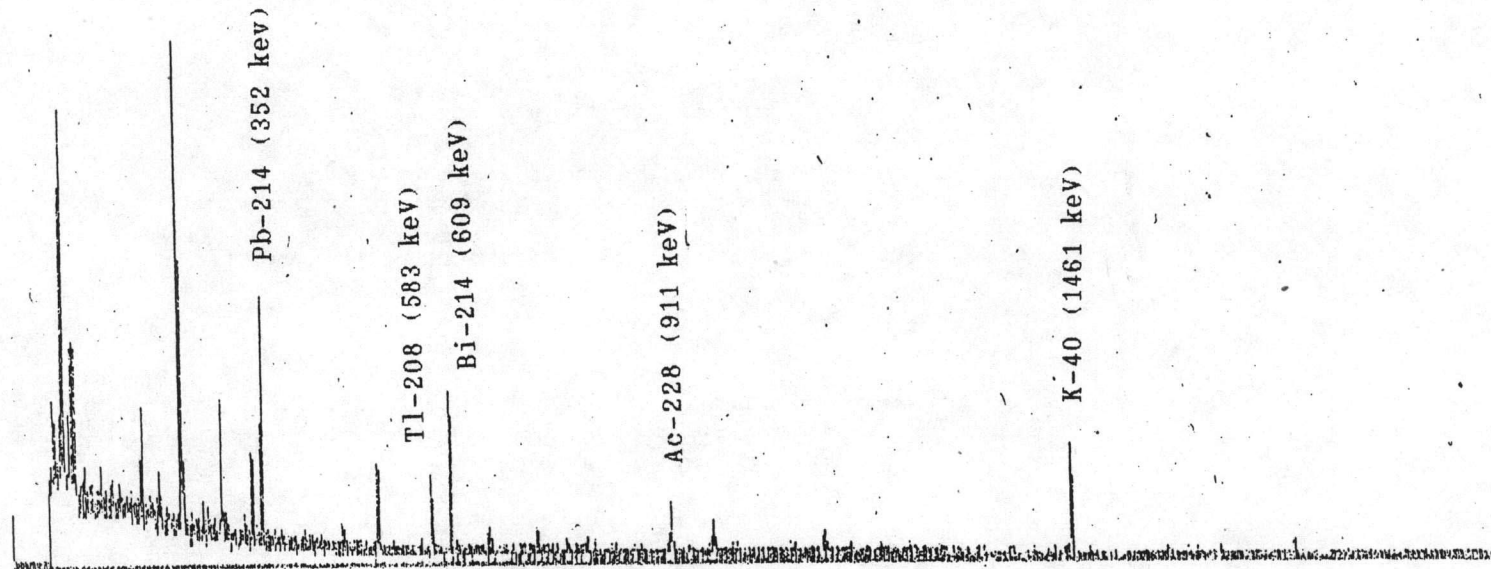
Figure 3.9 Gamma-ray Spectrum of Lignite Sample (Ash = 68.4%)

HFS: 0 - 4095

VFS: 1K

MIN/LOG

MAX/MANUAL



CL= CH# 2
COUNTS 0

FROM CH# 2
ROI# 0 INT 78782

TO CH# 4095
AREA 76735

PSET(L) 30000
ELAP(L) 29995

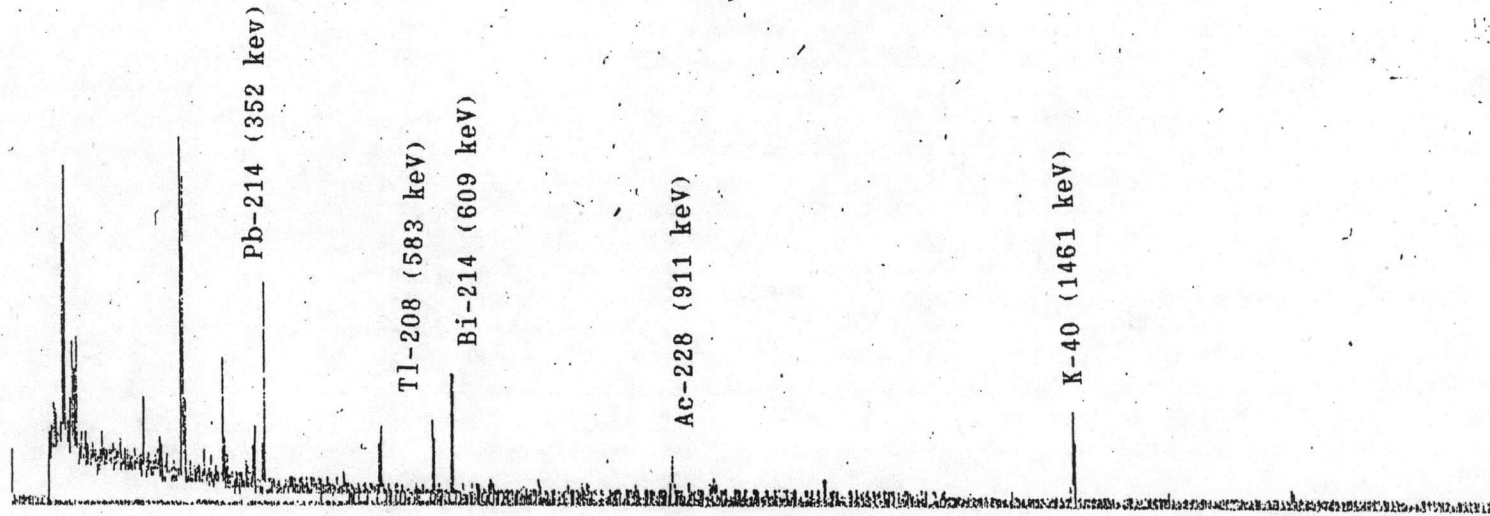
Figure 3.10 Gamma-ray Spectrum of Bottom Ash Collected on

25 November 1991

HFS: 0 - 4095

VFS: 1K

MIN/LOG TIME/MANUAL



CL= CH# 2
COUNTS 0

FROM CH# 2 TO CH# 4095
ROI# 0 INT 56860 AREA 53277

PSET(1) 18006
ELAP(1) 18012

Figure 3.11 Gamma-ray Spectrum of Fly Ash Collected on

25 November 1991

I 1031AA28